Supercapacitors Based on Flexible Graphene/Polyaniline Nanofiber Composite Films

Qiong Wu, Yuxi Xu, Zhiyi Yao, Anran Liu, and Gaoquan Shi*

Department of Chemistry and Laboratory of Bio-organic Phosphorus, Tsinghua University, Beijing 100084, People's Republic of China

ABSTRACT Composite films of chemically converted graphene (CCG) and polyaniline nanofibers (PANI-NFs) were prepared by vacuum filtration the mixed dispersions of both components. The composite film has a layered structure, and PANI-NFs are sandwiched between CCG layers. Furthermore, it is mechanically stable and has a high flexibility; thus, it can be bent into large angles or be shaped into various desired structures. The conductivity of the composite film containing 44% CCG (5.5×10^2 S m^{-1}) is about 10 times that of a PANI-NF film. Supercapacitor devices based on this conductive flexible composite film showed large electrochemical capacitance (210 F g^{-1}) at a discharge rate of 0.3 A g^{-1}. They also exhibited greatly improved electrochemical stability and rate performances.

KEYWORDS: graphene · polyaniline nanofiber · supercapacitor · composite · flexible

Graphene, a two-dimensional monolayer of sp^2-bonded carbon atoms, has attracted increasing attention in recent years,[1] mainly due to its extraordinarily high electrical and thermal conductivities,[2,3] great mechanical strength,[4] large specific surface area, and potentially low manufacturing cost.[5] Graphene has been explored for applications in fabricating electronic and energy storage devices,[6−8] sensors,[9,10] transparent electrodes,[11−13] supramolecular assemblies,[14,15] and nanocomposites.[16,17] In particular, the composites of graphene and polymers are of scientific and industrial interest because of their enhanced properties arising from the high conductivity and reinforcement of graphene nanofillers.[16,18,19]

On the other hand, conducting polymers (CPs) also have been extensively studied and widely applied in various organic devices.[20−25] To improve the performances or extend the functions of the devices, CPs usually have to be nanostructured.[23−25] Polyaniline (PANI) is a typical CP with good environmental stability, interesting electroactivity, and unusual doping/dedoping chemistry.[24,26−28] Nanostructured PANI can be synthesized through various chemical approaches.[23−25,29] For example, polyaniline-nanofibers (PANI-NFs) were facilely prepared by interfacial or rapid-mixing polymerization, and they have been applied for fabricating chemical sensors, actuators, memory devices, batteries, and supercapacitors.[24,30,31] However, chemically prepared nanostructured CPs including PANI-NF are usually powdery and insulating in their dedoped states.[26,32,33] Thus, various porous carbon materials (*e.g.*, activated carbon, mesoporous carbon, and carbon nanotubes) and a polymer binder (*e.g.*, Nafion) were usually used as additives for fabricating CP-based electrodes.[34−39] Graphene, as a new member of carbon nanomaterials, also has been applied for fabricating the composites with CPs.[40−43] Composites of PANI and graphene, graphite oxide, and graphene-based nanosheets or graphene paper were successfully prepared by *in situ* chemical or electrochemical polymerization, covalent or noncovalent functionalization, and self-assembly.[40,42,44−51] In most of the previous works, however, graphite oxide or graphene aggregates rather than stable dispersions of graphene sheets were used as the starting materials. However, graphite oxide is an insulator, and aggregated graphene sacrificed both large specific surface area and outstanding single-layer electric property of graphene.[52−54]

In this paper, we report a novel method for preparing the stable aqueous dispersions of CCG/PANI-NFs composites. By filtrating the mixed dispersions, paper-like composite films of CCG and PANI-NFs (G-PNF) were produced. In these films, PANI-NFs are uniformly sandwiched between CCG layers. Furthermore, the composite

*Address correspondence to gshi@mail.tsinghua.edu.cn

Received for review January 2, 2010 and accepted March 24, 2010.

Published online March 31, 2010. 10.1021/nn1000035

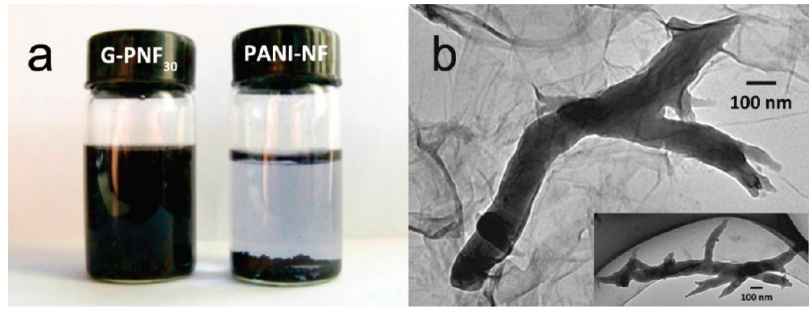

Figure 1. (a) G-PNF composite with r_G of 30% stably dispersed in an ammonia solution (pH = 9) (left) and pure PANI-NFs precipitated from the same medium after aging for 2 weeks (right). (a) TEM images of the G-PNF composite and pure PANI-NFs (inset).

film containing 44 wt % CCG exhibited greatly improved mechanical properties and conductivity in comparing with those of pure PANI-NF films. The supercapacitor based on this film possesses a high capacitance and has a high cycling stability.

RESULTS AND DISCUSSION

PANI-NFs used in this study were prepared by interfacial polymerization of aniline according to the literature.[33] The as-formed PANI-NFs were proved to be positively charged in their emeraldine salt form.[55] Thus, it was reported that as-formed PANI-NFs could form a stable composite dispersion with negatively charged oxidized carbon nanotubes (OCNTs) *via* electrostatic interaction.[56] On the other hand, CCG sheets also bring negative charges due to their residual carboxylic groups.[8] Therefore, it is expected that a stable composite dispersion of CCG and PANI-NFs also can be prepared through a similar process. However, CCG sheets are quite different from OCNTs mainly in two different aspects: first, CCG sheets have many more carboxylic groups located at their edges for electrostatic interaction.[8] Second, both OCNTs and PANI-NFs can be stably dispersed in the aqueous solutions with a pH value of 2.6.[55] However, CCG sheets can be stably dispersed only in a weak alkaline medium (pH = 10).[8] Mixing basic CCG and as-formed acidic PANI-NF dispersions (pH 10 and 2.6, respectively) will form a mixture with high salt concentration. The mixture was unstable and precipitated within several days as the weight ratio CCG/(PANI-NFs + CCG) (r_G) was higher than 3%. Furthermore, choosing a suitable pH value for one component would cause the aggregation of the other one. In particular, the aggregation of CCG was highly irreversible.[8,57] In order to solve this problem, we purified the as-formed PANI-NF dispersion by dialyzing it for 24 h to remove the excess ions and then mixed it with CCG colloid immediately to avoid aggregation (see the Methods section).

By mixing the purified PANI-NF dispersion with a controlled amount of CCG colloid (pH = 10) under sonication, a dark blue mixture with a pH value of about 9 was obtained. Surprisingly, the mixed dispersion was quite stable when its r_G was higher than 20% and only a small portion of the composite (<5%, by weight) was preticipated from the mixture as r_G was in the range of 20−40%. Composite dispersion was so stable that little precipitate was found after standing for over 1 month or centrifugation under 1500 rpm for 10 min (Figure 1a, left). In comparison, we adjusted the purified PANI-NF dispersion to pH = 9 with ammonia solution, and most PANI-NFs precipitated after aging for 2 weeks (Figure 1a, right).

Figure 1b shows the typical transmission electronic micrographs (TEM) of G-PNF composite and PANI-NFs. As can be seen from the inset of Figure 1b, PANI-NFs have an average diameter of about 120 nm and length of 0.5−3 μm, which are in agreement with those reported in the literature.[33] In the composite, PANI-NFs are coated or sandwiched by CCG sheets (Figure 1b). It is known that in alkaline medium (pH = 9) PANI-NFs are in their neutral state, while CCG sheets are negatively charged. As a result, CCG/PANI-NF nanocomposites also bring negative charges, and they can form a stable dispersion because of the electrostatic repulsion between each other. It should be noted here that we also found several naked PANI-NFs from the TEM images of the composite; however, they were usually precipitated upon aging or centrifugation treatment.[55]

By filtrating the mixed dispersions through a porous polytetraflouroethylene (PTFE) membrane, G-PNF composite films were prepared successfully. After treatment with aqueous HCl solution (0.1 mol L^{-1}), the PANI component in the film can be redoped; thus, the color of G-PNF films changed from dark blue to dark green. We found that the mechanical property of these films was crucially determined by the CCG weight content of the mixed dispersion (r_G). If r_G was too low (*e.g.*, 20%), the prepared composite film was fragile. When r_G was increased to 30%, a high-quality flexible film was obtained (Figure 2). As r_G was higher than 40%, the composite film shrunk dramatically after drying, possibly due to the regional aggregation of CCG sheets. Therefore, we chose the composite film with r_G of 30% (G-PNF_{30})

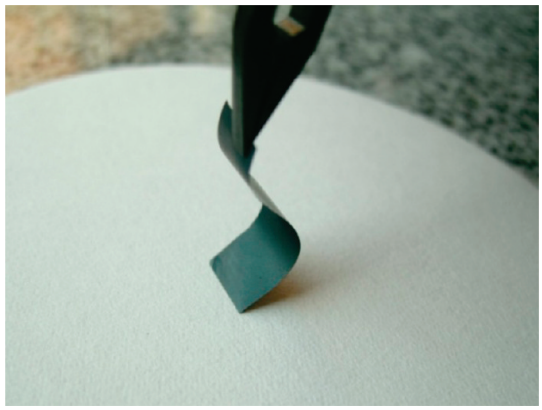

Figure 2. Digital photograph of a flexible G-PNF$_{30}$ film.

for further studies. The CCG content in G-PNF$_{30}$ was determined to be 44% by elemental analysis (Tables S1 and S2, Supporting Information), higher than the feeding r_G (30%). This is mainly due to the fact that the PANI-NFs of the mixed dispersion were partly lost during the process of filtration with cotton.

The G-PNF$_{30}$ film has a layered structure as shown in its cross-section scanning electron micrograph (SEM, Figure 3a), which is probably caused by the flow-assembly effect of graphene sheets during filtration.[58,59] The magnified SEM image (Figure 3b) reveals that PANI-NFs are sandwiched between CCG layers. The interspaces between the CCG layers are in the range of 10−200 nm. This morphology endows G-PNF$_{30}$ film with additional specific surface area comparing with that of the compact graphene film prepared under the same conditions (Figure 3c). Filtrating the dispersion of PANI-NFs also produced a porous film (Figure 3d). However, the mechanical property of this film is poor and it usually broke into small pieces after drying. Therefore, the G-PNF$_{30}$ film has several advantages over pure graphene or PANI-NF films for fabricating supercapacitors. First, the self-standing property and highly flexibility of G-PNF$_{30}$ film provide the possibility of shaping the material into desired structures by convenient mechanical techniques. Second, G-PNF$_{30}$ has a high conductivity of 5.5×10^2 S m^{-1}, which is about 10 times higher than that of pure PANI-NFs (50 S m^{-1}). Third, the composite film can be directly used for fabricating a supercapacitor device; neither an insulating binder nor a low capacitance conducting additive is required. Furthermore, as a flexible film, G-PNF$_{30}$ plays an irreplaceable role in fabricating flexible electronic devices such as roll-up displays, electronic papers, and intelligent cloths.[42]

The performances of the supercapacitor cells based on G-PNF$_{30}$ were evaluated by cyclic voltammetry (CV) and galvanostatic charge/discharge tests in two-electrode systems. Figure 4a illustrates the CV of a G-PNF$_{30}$ film and compares it with that of a CCG or a PANI-NF film with the same weight. The two pairs of redox waves shown in both CV of G-PNF$_{30}$ and PANI-NF films are attributed to the redox of PANI, corresponding to its leucoemeraldine/emeraldine and emeraldine/pernigraniline structural conversions, respectively. Both CVs have large rectangular areas, indicating these two supercapacitors have large double-layer capacitances. In comparison, the CV of CCG film exhibits a much smaller rectangular area, mainly due to its compact

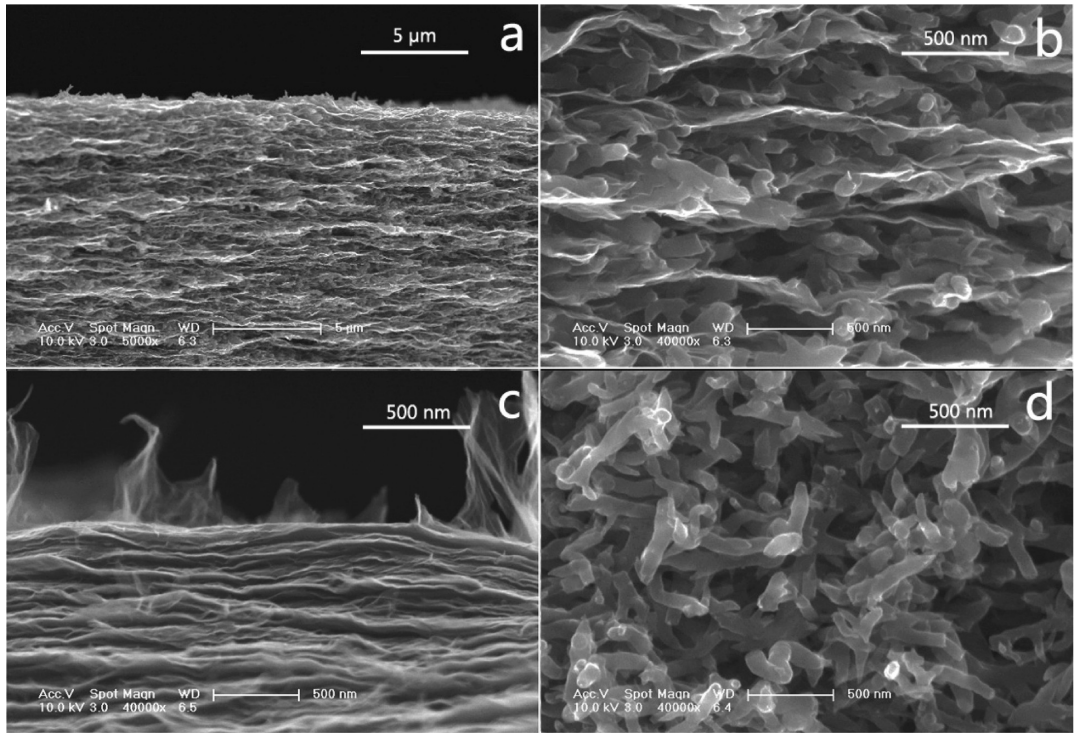

Figure 3. Cross-section SEM images of G-PNF$_{30}$ (a, b), pure CCG (c), and PANI-NF (d) films prepared by vacuum filtration.

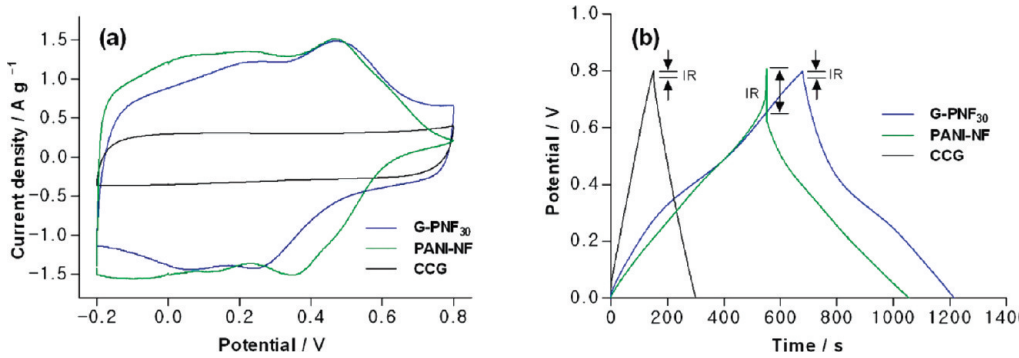

Figure 4. Cyclic voltammograms (a, scan rate = 5 mV s^{-1}) and galvanostatic charge/discharge curves (b, charging/discharging current density = 0.3 A g^{-1}) of the supercapacitors based on G-PNF$_{30}$, as-formed PANI-NF, and CCG films.

morphology and the absence of electroactive PANI component.[59]

Figure 4b demonstrates the galvanostatic charge/discharge curves of the supercapacitors tested at a charging/discharging current density of 0.3 A g^{-1}. All electrochemical tests of supercapacitors are based on two-electrode system, which can measure their performances more accurately.[7] The supercapacitor based on CCG films exhibited a triangular-shape charge/discharge curve, implying its capacitance is mainly attributed to pure electric double layer (EDL) capacitance. However, the discharging curve of the supercapacitor fabricated from G-PNF$_{30}$ films shows two voltage stages in the ranges of 0.8−0.45 V and 0.45−0 V, respectively. The former stage with a relatively short discharging duration is ascribed to EDL capacitance; nevertheless, the latter stage with a much longer discharging duration is associated with the combination of EDL and faradaic capacitances of PANI-NF component.[35] The discharge curve of the supercapacitor with PANI-NF films is similar to that of the supercapacitor with G-PNF$_{30}$ films. However, its "IR drop" is much higher than that of G-PNF$_{30}$ supercapacitor. This result reflects that the internal resistance of the former device is much higher than that of the latter.[60] Low internal resistance is of great importance in energy storing devices; for less energy will be wasted to produce unwanted heat during charging/discharging processes. Thus, G-PNF$_{30}$ film is more suitable for fabricating safe and power-saving supercapacitors compared with PANI-NF film.

Specific capacitances of G-PNF$_{30}$, PANI-NF, and CCG films calculated from their charge/discharge curves are listed in Table 1. It is clear from Table 1 that both the G-PNF$_{30}$ and PANI-NF films have much larger specific capacitances than CCG film. The gravimetric capacitance of G-PNF$_{30}$ film (210 F g^{-1}) is also much higher than the average value (arithmetic mean) of PANI-NF and CCG films (214 × 0.56 + 57 × 0.44 = 145 F g^{-1}), indicating the synergic effect of both components. This effect is mainly due to the following two factors. First, the incorporation of PANI-NFs into CCG greatly improved the double-layer capacitance of the composite film by forming a porous structure which has high specific surface area. The Brunauer−Emmett−Teller specific surface area test (BET-SSA, Table 1) shows that the specific surface area of G-PNF$_{30}$ is much higher than that of the CCG film. Second, the pseudocapacitance of PANI-NF in the composite film was enhanced by its highly conductive CCG component, which favors the redox reaction of PANI component. PANI in its leucoemeraldine or pernigraniline form is an insulator; thus, the supercapacitor based on PANI-NF films has a large internal resistance as it is fully charged or discharged. In G-PNF film, however, the CCG component has a conductance of as high as 4.0 × 10^3 S m^{-1}. Therefore, it forms a conducting network for improving the redox activity of PANI. Moreover, G-PNF$_{30}$ film possesses a much higher volumetric capacitance than that of PANI-NF film owing to its more compact structure, showing obvious merits in potential applications for low-volume high-capacitance devices.

The rate performance of G-PNF$_{30}$ film was evaluated by charging/discharging at different current densities (i_d) and compared with that of a PANI-NF film (Figure 5a). The G-PNF$_{30}$ film maintained its 94% capacitance (197 F g^{-1}) as i_d was increased from 0.3 to 3 A g^{-1}, while the PANI-NF film lost about 14% of its capacity in the same i_d range. This is possibly because the high conductivity of G-PNF$_{30}$ film accelerated its charge-transfer during the discharging process. However, when i_d was increased to be as high as 6 A g^{-1}, the specific capacitance of the G-PNF$_{30}$ film was measured to be slightly lower than that of the PANI-NF film. In this

TABLE 1. BET-SSA, Weight Density (ρ), and Gravimetric (C_m) and Volumetric (C_v) Capacitances of G-PNF$_{30}$, PANI-NF, and CCG Films (Measured at i_d = 0.3 A g^{-1})

film	BET-SSA/(m^2 g^{-1})	ρ/(g · cm^{-3})	C_m/(F · g^{-1})	C_v/(F · cm^{-3})
G-PNF$_{30}$	12.7	0.76	210	160
PANI-NF	34.4	0.54	214	116
CCG	very low	1.53	57	87

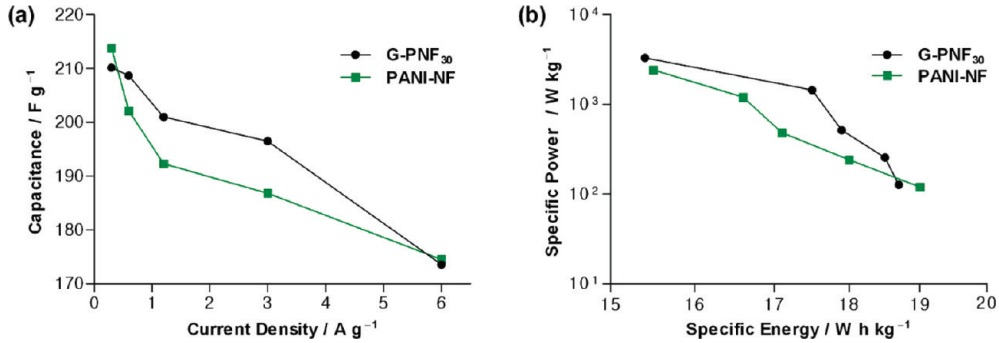

Figure 5. (a) Plots of specific capacitance *versus* discharging current density and (b) Ragone plots for G-PNF$_{30}$ and PANI-NF films.

case, the capacitances of both films were mainly limited by the diffusion of the supporting electrolyte. As a result, the smaller specific area of G-PNF$_{30}$ film made its capacitance dropped more dramatically at this discharge rate. It is also clear from Figure 5b that the G-PNF$_{30}$ film also has larger specific energy and specific power than those of the PANI-NF film as i_d was in the range of 0.6−6 A g^{-1}.

The Nyquist plots of G-PNF$_{30}$ and PANI-NF films are demonstrated in Figure 6. These plots do not show semicircle regions, probably due to the low faradaic resistances of the films. The 45° region in the plot of the PANI-NF film is short (50−10 Hz, Figure 7 inset), indicating a typical Warburg impedance. However, the 45° region in the plot of the G-PNF$_{30}$ film is quite long (from 1 kHz to 0.3 Hz). This result is accorded with the "transmission line" behavior, reflecting that the G-PNF$_{30}$ film has a porous structure as confirmed by its SEM images (Figure 3b).[61−63]

The instability of the capacitors based on CP films (especially PANI) during long-term charge/discharge cycling is one of their most lethal deficiencies. As shown in Figure 7, the capacitance of pure PANI-NF lost 29% (from 187 to 133 F g^{-1}) after 800 charging/discharging cycles at a current density of 3 A g^{-1}. However, under the same conditions, the capacitance of the G-PNF$_{30}$ film decreased only 21% (from 198 to 155 F g^{-1}). The improved electrochemical stability of the G-PNF$_{30}$ film can be explained as follows. In the composite, CCG sheets act as the frameworks for sustaining PANI-NFs, preventing the fibers from severely swelling and shrinking during cycling. Thus, the morphological and electrochemical property changes of PANI-NFs induced by charge/discharge cycling were greatly reduced.[64]

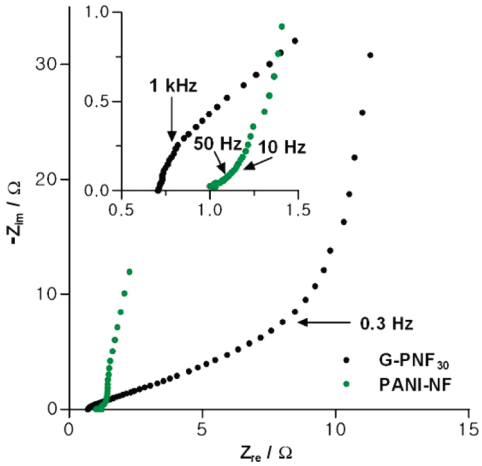

Figure 6. Nyquist plots of G-PNF$_{30}$ and PANI-NF films. Inset shows the magnified high-frequency regions.

CONCLUSIONS

Stable aqueous dispersions of CCG/PANI-NF composite have been successfully prepared by mixing two purified components with the assistance of ultrasonication. This method provided a new route to graphene-based nanocomposites. Free-standing, flexible G-PNF$_{30}$ composite film with layered structure was obtained *via* filtration of the aqueous dispersion of the composite. The conductivity of G-PNF$_{30}$ film was measured to be as high as 5.5 × 10^2 S m^{-1}, which is one order higher than that of pure PANI-NF film. The symmetric supercapacitor device using G-PNF$_{30}$ films was successful as both electrodes exhibited a high capacitance of 210 F g^{-1} (or 160 F cm^{-3}) at 0.3 A g^{-1}, and this capacitance can be maintained for about 94% (197 F g^{-1}) as the discharging current density was increased from 0.3 to

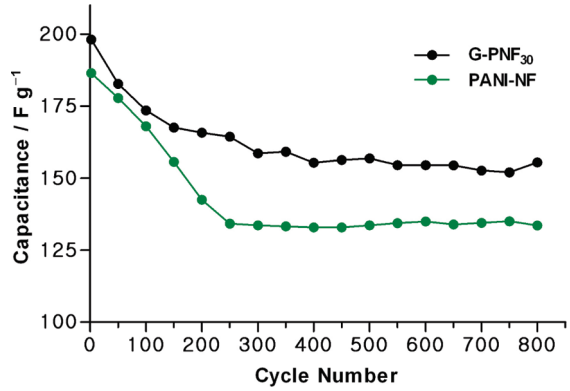

Figure 7. Cycling stability of G-PNF$_{30}$ and PANI-NF films upon charging/discharging at a current density of 3 A g^{-1}.

3 A g^{-1}. Furthermore, the G-PNF_{30}-based capacitor has good stability so that after 800 charging/discharging cycles at current density of 3 A g^{-1} a high capacitance of 155 F g^{-1} was maintained. These performances are much higher than those of the supercapacitors based on pure CCG or PANI-NF films, mainly due to the synergic effect of both components.

METHODS

Preparation of Graphite Oxide (GO) and CCG Colloids. GO was prepared by Hummer's method[65] and purified by dialysis, and the details are described in the literature.[14] Graphene colloid was prepared by an electrostatic stabilization method developed by Li and co-workers.[8] The procedures are described briefly as follows. Purified GO (1 mg mL^{-1}) was centrifuged under 3000 rpm to remove aggregates and then diluted to 0.4 mg mL^{-1}. Successively, 1.05 mL of ammonia solution (25%, Beijing Chem. Works) and 132 μL of hydrazine monohydrate (99%, Alfa Aesar) were added into 300 mL of diluted GO dispersion, mixed by vigorous shaking for 1 min, and then kept at 95 °C for 1 h. The resulting solution was filtered through cotton and dialyzed against ammonia solution (pH = 10) for one week. Finally, the dispersion was centrifuged under 3000 rpm for 20 min to remove aggregated graphene sheets.

Preparation and Purification of PANI-NFs. PANI-NFs were prepared by interfacial polymerization reported by Huang and coworkers,[33] and the procedures are briefly described as follows. In a 30 mL glass vial, 0.585 mL of freshly distilled aniline (Beijing Chemical Reagent Co.) was dissolved in 10 mL of chloroform (Tianjin Third Chemical Reagent Co.). $HClO_4$ (1.65 mL, 70%, Tianjin Xinyuan Chemical Co.) and ammonia persulfate (0.365 g, AR, Sinopharm Chemical Reagent Co.) were dissolved in 20 mL of deionized water and then carefully transported into the aniline solution described above to form a stable interface. Polymerization was performed in the dark at room temperature overnight. After polymerization, the aqueous phase was collected and purified by dialysis. In this process, 20 mL of the suspension was dialyzed against 1 L of deionized water under stirring for about 24 h until its pH value was higher than 6. The concentration of PANI-NF dispersion was calibrated immediately and then used for mixing with CCG colloid as soon as possible (within 12 h). Otherwise, aggregated PANI-NFs will be formed in the neutral medium, which will reduce the quality of the G-PNF composite.[55]

Preparation of G-PNF Composite Films. The structures and compositions of CCG and PANI-NF were confirmed by X-ray photoelectron spectroscopy and elemental analysis (Figure S1 and Table S1, Supporting Information). PANI-NF was diluted to 0.3 mg mL^{-1} with deionized water and redispersed by sonication (using a 180 W ultrasonication cleaner) for 0.5 h. Then, graphene colloid (0.2 mg mL^{-1}) was added, and the resulting mixture was sonicated for another 2 h. The composition of the composite was controlled by the volume ratio of the two suspensions. After filtration with cotton to remove the trace amount of precipitate, the mixture was carefully poured into a vacuum filter equipped with a 0.22 μm porous PTFE membrane and filtered under low pressure (0.04 MPa) to produce a composite film. Then, the composite film was immersed in an aqueous solution of 0.1 M HCl overnight to redope its PANI-NF component. Finally, it was dried under vacuum at room temperature. For control experiments, PANI-NF colloid was also prepared by redispersing purified PANI-NFs in aqueous HCl solution (pH = 2.6). PANI-NF colloid or CCG sheets were filtrated under vacuum to produce corresponding films. It should be noted here that the mechanical property of PANI-NF film is poor, and it usually broke into several small pieces after drying.

Characterizations. Scanning and transmission electron micrographs were recorded on a Sirion 200s scanning electron microscope (JEOL) and a 7650B transmission electron microscope (Hitachi), respectively. Conductivities of the films were measured by a conventional four-probe technique. The BET surface area was measured by using a QuadraSorb SI surface area analyzer (Quantachrome Instrument). The structure of the supercapacitor cells is shown in Figure 8, and the procedures of fabricating the devices are described as follows. Two pieces of G-PNF_{30}, PANI-NF, or CCG films were used as both electrodes, and they were separated by a filtrate paper soaked with electrolyte (1 M H_2SO_4). Two Pt foils were used as the current collectors. All of the components were assembled into a layered structure and sandwiched between two pieces of glass slides.[7,66] A flexible supercapacitor can also be fabricated by replacing glass slides with plastic sheets and using flexible carbon-based current collectors.

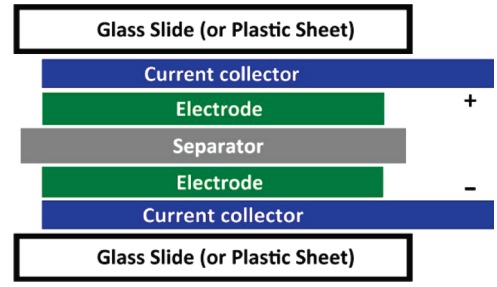

Figure 8. Schematic illustration of a supercapacitor cell.

Electrochemical performances of the supercapacitor cells were tested by cyclic voltammetry (CV), galvanostatic charge/discharge (on a CHI 440 potentiostat, CH Instruments, Inc.), and electrochemical impedance spectroscopy (EIS, on a CHI 660 potentiostat, CH Instruments, Inc.). All of the experiments were carried out in a two-electrode system. The potential range for CV examinations was −0.2 to +0.8 V, and that for galvanostatic charge/discharge tests was 0−0.8 V. EIS tests were carried out in the frequency range of 10^5−0.05 Hz at a 10 mV amplitude referring to open circuit potential. The mass and volume specific capacitances (C_m and C_v, respectively) were calculated by using the equations $C_m = (I\Delta t)/(m\Delta V)$ and $C_V = C_m\rho$, where I is the constant discharge current, Δt is the discharging time, m is the total mass of the electrode, ΔV is the voltage drop upon discharging (excluding the IR drop), and ρ is the density of the film. Specific energy (E) and specific power (P) in the Ragone plot were calculated by using the equations $E = {}^1/_2 C_m \Delta V^2$ and $P = E/\Delta t$, respectively.

Acknowledgment. This work was supported by the National Natural Science Foundation of China (50873052, 20774056, and 50533030) and the Open Research Fund of State Key Lab of Bioelectronics of China.

Supporting Information Available: X-ray photoelectron spectroscopy characterization and elemental analysis details of G-PNF_{30}, PANI-NF, and CCG. This material is available free of charge *via* the Internet at http://pubs.acs.org.

REFERENCES AND NOTES

1. Novoselov, K. S.; Geim, A. K.; Morozov, S. V.; Jiang, D.; Zhang, Y.; Dubonos, S. V.; Grigorieva, I. V.; Firsov, A. A. Electric Field Effect in Atomically Thin Carbon Films. *Science* **2004**, *306*, 666–669.
2. Geim, A. K.; Novoselov, K. S. The Rise of Graphene. *Nat. Mater.* **2007**, *6*, 183–191.
3. Balandin, A. A.; Ghosh, S.; Bao, W. Z.; Calizo, I.; Teweldebrhan, D.; Miao, F.; Lau, C. N. Superior Thermal Conductivity of Single-Layer Graphene. *Nano Lett.* **2008**, *8*, 902–907.
4. Lee, C.; Wei, X. D.; Kysar, J. W.; Hone, J. Measurement of the Elastic Properties and Intrinsic Strength of Monolayer Graphene. *Science* **2008**, *321*, 385–388.

5. Park, S.; Ruoff, R. S. Chemical Methods for the Production of Graphenes. *Nat. Nanotechnol.* **2009**, *4*, 217–224.
6. Liang, M. H.; Zhi, L. J. Graphene-Based Electrode Materials for Rechargeable Lithium Batteries. *J. Mater. Chem.* **2009**, *19*, 5871–5878.
7. Stoller, M. D.; Park, S. J.; Zhu, Y. W.; An, J. H.; Ruoff, R. S. Graphene-Based Ultracapacitors. *Nano Lett.* **2008**, *8*, 3498–3502.
8. Li, D.; Muller, M. B.; Gilje, S.; Kaner, R. B.; Wallace, G. G. Processable Aqueous Dispersions of Graphene Nanosheets. *Nat. Nanotechnol.* **2008**, *3*, 101–105.
9. Fowler, J. D.; Allen, M. J.; Tung, V. C.; Yang, Y.; Kaner, R. B.; Weiller, B. H. Practical Chemical Sensors from Chemically Derived Graphene. *ACS Nano* **2009**, *3*, 301–306.
10. Robinson, J. T.; Perkins, F. K.; Snow, E. S.; Wei, Z. Q.; Sheehan, P. E. Reduced Graphene Oxide Molecular Sensors. *Nano Lett.* **2008**, *8*, 3137–3140.
11. Vollmer, A.; Feng, X. L.; Wang, X.; Zhi, L. J.; Mullen, K.; Koch, N.; Rabe, J. P. Electronic and Structural Properties of Graphene-Based Transparent and Conductive Thin Film Electrodes. *Appl. Phys. A: Mater. Sci. Process.* **2009**, *94*, 1–4.
12. Becerril, H. A.; Mao, J.; Liu, Z.; Stoltenberg, R. M.; Bao, Z.; Chen, Y. Evaluation of Solution-processed Reduced Graphene Oxide Films as Transparent Conductors. *ACS Nano* **2008**, *2*, 463–470.
13. Hong, W. J.; Xu, Y. X.; Lu, G. W.; Li, C.; Shi, G. Q. Transparent Graphene/PEDOT-PSS Composite Films as Counter Electrodes of Dye-sensitized Solar Cells. *Electrochem. Commun.* **2008**, *10*, 1555–1558.
14. Xu, Y. X.; Zhao, L.; Bai, H.; Hong, W. J.; Li, C.; Shi, G. Q. Chemically Converted Graphene Induced Molecular Flattening of 5,10,15,20-Tetrakis(1-methyl-4-pyridinio)porphyrin and Its Application for Optical Detection of Cadmium(II) Ions. *J. Am. Chem. Soc.* **2009**, *131*, 13490–13497.
15. Xu, Y. X.; Bai, H.; Lu, G. W.; Li, C.; Shi, G. Q. Flexible Graphene Gilms *via* the Filtration of Water-Soluble Noncovalent Functionalized Graphene Sheets. *J. Am. Chem. Soc.* **2008**, *130*, 5856–5857.
16. Stankovich, S.; Dikin, D. A.; Dommett, G. H. B.; Kohlhaas, K. M.; Zimney, E. J.; Stach, E. A.; Piner, R. D.; Nguyen, S. T.; Ruoff, R. S. Graphene-Based Composite Materials. *Nature* **2006**, *442*, 282–286.
17. Xu, Y. X.; Hong, W. J.; Bai, H.; Li, C.; Shi, G. Q. Strong and Ductile Poly(vinyl alcohol)/Graphene Oxide Composite Films with a Layered Structure. *Carbon* **2009**, *47*, 3538–3543.
18. Rao, C. N. R.; Sood, A. K.; Subrahmanyam, K. S.; Govindaraj, A. Graphene: The New Two-Dimensional Nanomaterial. *Angew. Chem., Int. Ed.* **2009**, *48*, 7752–7777.
19. Fang, M.; Wang, K. G.; Lu, H. B.; Yang, Y. L.; Nutt, S. Covalent Polymer Functionalization of Graphene Nanosheets and Mechanical Properties of Composites. *J. Mater. Chem.* **2009**, *19*, 7098–7105.
20. Schultze, J. W.; Karabulut, H. Application Potential of Conducting Polymers. *Electrochim. Acta* **2005**, *50*, 1739–1745.
21. Li, C.; Bai, H.; Shi, G. Q. Conducting Polymer Nanomaterials: Electrosynthesis and Applications. *Chem. Soc. Rev.* **2009**, *38*, 2397–2409.
22. Lu, G. W.; Hong, W. J.; Tong, L.; Bai, H.; Wei, Y.; Shi, G. Q. Drying Enhanced Adhesion of Polythiophene Nanotubule Arrays on Smooth Surfaces. *ACS Nano* **2008**, *2*, 2342–2348.
23. Tran, H. D.; Li, D.; Kaner, R. B. One-Dimensional Conducting Polymer Nanostructures: Bulk Synthesis and Applications. *Adv. Mater.* **2009**, *21*, 1487–1499.
24. Li, D.; Huang, J. X.; Kaner, R. B. Polyaniline Nanofibers: A Unique Polymer Nanostructure for Versatile Applications. *Acc. Chem. Res.* **2009**, *42*, 135–145.
25. Wan, M. X. A Template-Free Method Towards Conducting Polymer Nanostructures. *Adv. Mater.* **2008**, *20*, 2926–2932.
26. Bai, H.; Shi, G. Q. Gas Sensors Based on Conducting Polymers. *Sensors* **2007**, *7*, 267–307.
27. Kang, E. T.; Neoh, K. G.; Tan, K. L. Polyaniline: A Polymer with Many Interesting Intrinsic Redox States. *Prog. Polym. Sci.* **1998**, *23*, 277–324.
28. Ryu, K. S.; Kim, K. M.; Park, N. G.; Park, Y. J.; Chang, S. H. Symmetric Redox Supercapacitor with Conducting Polyaniline Electrodes. *J. Power Sources* **2002**, *103*, 305–309.
29. Bhadra, S.; Khastgir, D.; Singha, N. K.; Lee, J. H. Progress in Preparation, Processing and Applications of Polyaniline. *Prog. Polym. Sci.* **2009**, *34*, 783–810.
30. Huang, J. X.; Kaner, R. B. Nanofiber Formation in the Chemical Polymerization of Aniline: A Mechanistic Study. *Angew. Chem., Int. Ed.* **2004**, *43*, 5817–5821.
31. Huang, J. X.; Virji, S.; Weiller, B. H.; Kaner, R. B. Polyaniline Nanofibers: Facile Synthesis and Chemical Sensors. *J. Am. Chem. Soc.* **2003**, *125*, 314–315.
32. Huang, J. X.; Kaner, R. B. The Intrinsic Nanofibrillar Morphology of Polyaniline. *Chem. Commun.* **2006**, 367–376.
33. Huang, J. X.; Kaner, R. B. A General Chemical Route to Polyaniline Nanofibers. *J. Am. Chem. Soc.* **2004**, *126*, 851–855.
34. Jang, J.; Bae, J.; Choi, M.; Yoon, S. H. Fabrication and Characterization of Polyaniline Coated Carbon Nanofiber for Supercapacitor. *Carbon* **2005**, *43*, 2730–2736.
35. Li, L. X.; Song, H. H.; Zhang, Q. C.; Yao, J. Y.; Chen, X. H. Effect of Compounding Process on the Structure and Electrochemical Properties of Ordered Mesoporous Carbon/Polyaniline Ccomposites as Electrodes for Supercapacitors. *J. Power Sources* **2009**, *187*, 268–274.
36. Park, J. H.; Park, O. O. Hybrid Electrochemical Capacitors Based on Polyaniline and Activated Carbon Electrodes. *J. Power Sources* **2002**, *111*, 185–190.
37. Peng, C.; Zhang, S. W.; Jewell, D.; Chen, G. Z. Carbon Nanotube and Conducting Polymer Composites for Supercapacitors. *Prog. Nat. Sci.* **2008**, *18*, 777–788.
38. Zhang, J.; Kong, L. B.; Wang, B.; Luo, Y. C.; Kang, L. In-Situ Electrochemical Polymerization of Multi-Walled Carbon Nanotube/Polyaniline Composite Films for Electrochemical Supercapacitors. *Synth. Met.* **2009**, *159*, 260–266.
39. Zhang, L. L.; Li, S.; Zhang, J.; Guo, P.; Zheng, J.; Zhao, X. S. Enhancement of Electrochemical Performance of Macroporous Carbon by Surface Coating of Polyaniline. *Chem. Mater.* **2010**, *22*, 1195–1202.
40. Yan, J.; Wei, T.; Shao, B.; Fan, Z.; Qian, W.; Zhang, M.; Wei, F. Preparation of a Graphene Nanosheet/Polyaniline Composite with High Specific Capacitance. *Carbon* **2010**, *48*, 487–493.
41. Wang, Y.; Shi, Z. Q.; Huang, Y.; Ma, Y. F.; Wang, C. Y.; Chen, M. M.; Chen, Y. S. Supercapacitor Devices Based on Graphene Materials. *J. Phys. Chem. C* **2009**, *113*, 13103–13107.
42. Wang, D. W.; Li, F.; Zhao, J. P.; Ren, W. C.; Chen, Z. G.; Tan, J.; Wu, Z. S.; Gentle, I.; Lu, G. Q.; Cheng, H. M. Fabrication of Graphene/Polyaniline Composite Paper *via In Situ* Anodic Electropolymerization for High-Performance Flexible Electrode. *ACS Nano* **2009**, *3*, 1745–1752.
43. Rao, C. N. R.; Subrahmanyam, K. S.; Biswas, K.; Govindaraj, A. Graphene, The New Nanocarbon. *J. Mater. Chem.* **2009**, *19*, 2457–2469.
44. Zhao, L.; Zhao, L.; Xu, Y.; Qiu, T.; Zhi, L.; Shi, G. Polyaniline Electrochromic Devices With Transparent Graphene Electrodes. *Electrochim. Acta* **2009**, *55*, 491–497.
45. Liu, Y. S.; Zhou, J. Y.; Zhang, X. L.; Liu, Z. B.; Wan, X. J.; Tian, J. G.; Wang, T.; Chen, Y. S. Synthesis, Characterization and Optical Limiting Property of Covalently Oligothiophene-Functionalized Graphene Material. *Carbon* **2009**, *47*, 3113–3121.
46. Bai, H.; Xu, Y. X.; Zhao, L.; Li, C.; Shi, G. Q. Non-Covalent Functionalization of Graphene Sheets by Sulfonated Polyaniline. *Chem. Commun.* **2009**, 1667–1669.
47. Xiao, P.; Xiao, M.; Liu, P. G.; Gong, K. C. Direct Synthesis of a Polyaniline-Intercalated Graphite Oxide Nanocomposite. *Carbon* **2000**, *38*, 626–628.

48. Wang, H. L.; Hao, Q. L.; Yang, X. J.; Lu, L. D.; Wang, X. Graphene Oxide Doped Polyaniline for Supercapacitors. *Electrochem. Commun.* **2009**, *11*, 1158–1161.
49. Liu, P. G.; Gong, K. C. Synthesis of Polyaniline-Intercalated Graphite Oxide by an *In Situ* Oxidative Polymerization Reaction. *Carbon* **1999**, *37*, 706–707.
50. Higashika, S.; Kimura, K.; Matsuo, Y.; Sugie, Y. Synthesis of Polyaniline-Intercalated Graphite Oxide. *Carbon* **1999**, *37*, 354–356.
51. Bissessur, R.; Liu, P. K. Y.; White, W.; Scully, S. F. Encapsulation of Polyanilines into Graphite Oxide. *Langmuir* **2006**, *22*, 1729–1734.
52. Wang, D.-W.; Li, F.; Wu, Z.-S.; Ren, W.; Cheng, H.-M. Electrochemical Interfacial Capacitance in Multilayer Graphene Sheets: Dependence on Number of Stacking Layers. *Electrochem. Commun.* **2009**, *11*, 1729–1732.
53. Stankovich, S.; Dikin, D.; Piner, R.; Kohlhaas, K.; Kleinhammes, A.; Jia, Y.; Wu, Y.; Nguyen, S.; Ruoff, R. Synthesis of Graphene-Based Nanosheets *via* Chemical Reduction of Exfoliated Graphite Oxide. *Carbon* **2007**, *45*, 1558–1565.
54. Li, X. L.; Zhang, G. Y.; Bai, X. D.; Sun, X. M.; Wang, X. R.; Wang, E.; Dai, H. J. Highly Conducting Graphene Sheets and Langmuir-Blodgett Films. *Nat. Nanotechnol.* **2008**, *3*, 538–542.
55. Li, D.; Kaner, R. B. Processable Stabilizer-Free Polyaniline Nanofiber Aqueous Colloids. *Chem. Commun.* **2005**, 3286–3288.
56. Yan, X. B.; Han, Z. J.; Yang, Y.; Tay, B. K. Fabrication of Carbon Nanotube-Polyaniline Composites *via* Electrostatic Adsorption in Aqueous Colloids. *J. Phys. Chem. C* **2007**, *111*, 4125–4131.
57. Chen, Y.; Zhang, X.; Yu, P.; Ma, Y. W. Stable Dispersions of Graphene and Highly Conducting Graphene Films: a New Approach to Creating Colloids of Graphene Monolayers. *Chem. Commun.* **2009**, 4527–4529.
58. Dikin, D. A.; Stankovich, S.; Zimney, E. J.; Piner, R. D.; Dommett, G. H. B.; Evmenenko, G.; Nguyen, S. T.; Ruoff, R. S. Preparation and Characterization of Graphene Oxide Paper. *Nature* **2007**, *448*, 457–460.
59. Chen, H.; Muller, M. B.; Gilmore, K. J.; Wallace, G. G.; Li, D. Mechanically Strong, Electrically Conductive, and Biocompatible Graphene Paper. *Adv. Mater.* **2008**, *20*, 3557–3561.
60. Hu, L.; Choi, J. W.; Yang, Y.; Jeong, S.; La Mantia, F.; Cui, L.-F.; Cui, Y. Highly Conductive Paper for Energy-storage Devices. *Proc. Natl. Acad. Sci. U.S.A.* **2009**, *106*, 21490–21494.
61. Li, L. X.; Song, H. H.; Chen, X. H. Pore Characteristics and Electrochemical Performance of Ordered Mesoporous Carbons for Electric Double-Layer Capacitors. *Electrochim. Acta* **2006**, *51*, 5715–5720.
62. de Levie, R. On Porous Electrodes in Electrolyte Solutions: I. Capacitance Effects. *Electrochim. Acta* **1963**, *8*, 751–780.
63. Conway, B. E.; Birss, V.; Wojtowicz, J. The Role and Utilization of Pseudocapacitance for Energy Storage by Supercapacitors. *J. Power Sources* **1997**, *66*, 1–14.
64. Kotz, R.; Carlen, M. Principles and Applications of Electrochemical Capacitors. *Electrochim. Acta* **2000**, *45*, 2483–2498.
65. Hummers, W. S.; Offeman, R. E. Preparation of Graphitic Oxide. *J. Am. Chem. Soc.* **1958**, *80*, 1339.
66. Nystrom, G.; Razaq, A.; Stromme, M.; Nyholm, L.; Mihranyan, A. Ultrafast All-Polymer Paper-Based Batteries. *Nano Lett.* **2009**, *9*, 3635–3639.